A control oriented guided tour in oilwell drilling vibration modeling

Martha Belem Saldivar, Sabine Mondié, Silviu-Iulian Niculescu, Hugues Mounier, Islam Boussaada

A control oriented guided tour in oilwell drilling vibration modeling

B. Saldivar[a,*], S. Mondié[b], S.-I. Niculescu[c], H. Mounier[c], I. Boussaada[c]

[a] *CONACYT - Facultad de Ingeniería - Universidad Autónoma del Estado de México, Instituto Literario No. 100 Ote., 50130 Toluca, Edo. de México, Mexico*
[b] *Departamento de Control Automático CINVESTAV-IPN, Av. IPN No. 2508, Col. San Pedro Zacatenco, C.P. 07360, México D.F., Mexico*
[c] *Laboratoire des Signaux et Systèmes (L2S, UMR CNRS 8506), CNRS-Centrale Supélec-Université Paris-Sud, Gif-sur-Yvette, France*

Abstract

In drilling operations, the interaction of the drillstring with the borehole leads to vibrations affecting the performance and increasing the drilling cost. The development of controllers to get a faster and efficient drilling operation is based on a mathematical modeling allowing a proper system characterization and the identification of the vibration sources to avoid them or mitigate their influence. This paper presents an overview of the modeling of axial and torsional self-excited drilling vibrations.

Keywords: self-excited drilling vibrations, stick-slip, bit-bounce, lumped parameter models, distributed parameter models, wave equation, frictional torque

1. Introduction

Self-excited drillstring vibrations are the main cause of loss of performance in the perforation process for oil and gas; they provoke premature wear and tear of drilling equipment resulting in fatigue and induced failures such as pipe wash-out

*Corresponding author
Email addresses: mbsaldivarma@conacyt.mx (B. Saldivar), smondie@ctrl.cinvestav.mx (S. Mondié), silviu.niculescu@lss.supelec.fr (S.-I. Niculescu), hugues.mounier@lss.supelec.fr (H. Mounier), islam.boussaada@lss.supelec.fr (I. Boussaada)

and twist-off [53]. Besides, they may cause significant wastage of drilling energy [52] and may induce wellbore instabilities reducing the directional control and its overall shape [26]. In the oil industry, the improvement of drilling performance is a matter of crucial economical interest.

Self-excited vibrations can be explained by the instability of an equilibrium in the dynamic system description (see e.g. [45]). An unstable equilibrium point implies that a small initial system perturbation will grow over time until it manifests itself as the observable phenomena of stick-slip, in the case of torsional vibrations, or bit-bouncing, in the case of axial vibrations [2], [20], [33] . The bit-bounce phenomenon, caused by axial vibrations, is characterized by a repetitive loss of contact of the bit with the rock formation. The stick-slip effect, provoked by torsional vibrations, can be recognized by the successive occurrence of two phases: *stick* (the bit stops rotating) and *slip* (the bit is released from the stick phase with angular velocity higher than the nominal one) [43]. It has been documented that the stick-slip phenomenon occurs for about fifty percent of the drilling operation [40].

The harmful consequences of drillstring vibrations have motivated extensive research to analyze them and to try to mitigate their influence during drilling operations. In order to reduce the costs of failures, extensive research effort has been conducted in the last five decades to suppress the drillstring vibrations; several methodologies have been proposed, both from practical and theoretical viewpoints, see for example the references cited in the survey [48] and in [36].

Even though numerous studies to avoid drilling vibrations have been carried out and new technology has been deployed, such phenomena still occurs, significantly affecting on drilling costs and daily operations.

This paper enhances the contributions [10], [67] with a compilation of the main modeling techniques to reproduce the drillstring axial-torsional behavior and with a review of the most popular models to describe bit-rock friction forces. It is organized as follows: Section 2 presents the different modeling strategies to reproduce torsional and axial vibrations; existing models can be classified into four categories: lumped parameter models, distributed parameter models,

neutral-type time-delay models and PDE-ODE models. Important remarks allowing a comparison between the modeling approaches are provided. Section 3 reviews the most popular techniques used to describe the friction forces leading to the occurrence of drilling vibrations. Section 4 presents simulation results of the drilling system subject to different bit-rock frictional interface models. Finally, conclusions are presented in Section 5.

2. Drillstring models

A sketch of a simplified drillstring system is shown in Figure 1.

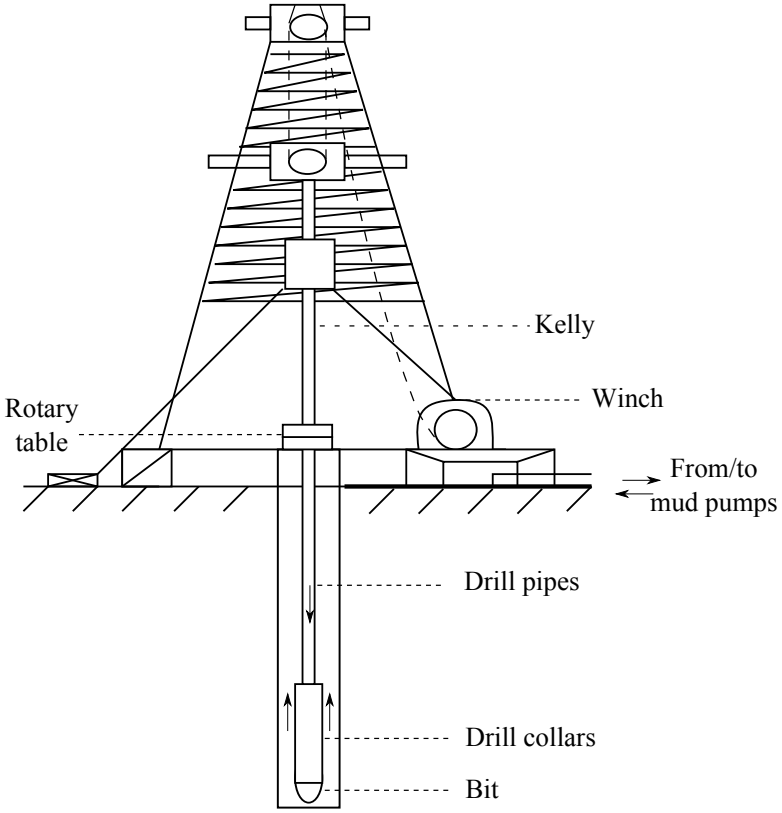

Figure 1: Basic scheme of a vertical drilling system.

Roughly speaking, the main components of a drilling system, called a *drilling*

rig, consist in drill pipes, steel tubes of typically 10 meters length; *drill collars*, much thicker pipes which provide the necessary weight to perform the perforation; *stabilizers*, which are thicker drill collars whose purpose is to avoid lateral motion of the drill pipes; and a rock cutting device, usually known as *bit*. The whole set is called *drillstring*, which is rotated through the rotary table located at the top. All the pipes of the drillstring are hollow, so that a drilling fluid can be injected by a mud pump in order to evacuate the removed rock. The set of drill collars, stabilizers and the bit is called *Bottom Hole Assembly* (BHA).

Modeling of drillstring dynamics constitutes the basis for system analysis and control of harmful vibrations. Over the last half-century, extensive research effort has been conducted to mathematically describe the physical phenomena occurring in real wells.

Existing drilling models can be classified into the following general categories:

- **Lumped parameter models.** The drillstring is regarded as a mass-spring-damper system which can be described by an ordinary differential equation. This finite-dimensional system representation provides a rough description of the dynamics taking place at different levels of the string; it can be of one to several degrees of freedom.

- **Distributed parameter models.** The drillstring is considered as a beam subject to axial and/or torsional efforts. A system of partial differential equations provides a characterization of the drilling variables in an infinite-dimensional setting. The price paid for the model accuracy is the complexity involved in its analysis and simulations.

- **Neutral-type time-delay models.** These models, which are directly derived from the distributed parameter ones (when damping is considered negligible), provide an input-output system description. The involved time-delays (which are dependent on the string length) are related to the speed of the oscillatory waves traveling throughout the rod. This type of model provides a good trade-off between system representation accuracy and complexity of the description.

– **Coupled PDE-ODE models.** Due to the great interest in the design of controllers for eliminating drilling vibrations, in recent years, researchers in the control area have developed modeling transformations that facilitate the design of stabilizing controllers. Most of the proposed techniques are based on different changes of variables applied to the wave equation describing the propagating waves along the drillstring, this allows describing the system through a set of coupled PDE-ODE equations.

2.1. Lumped parameter models

2.1.1. Torsional dynamics

The use of reduced models for vibration analysis is motivated by the need to define a simple description of drilling dynamics. Roughly speaking, the continuous system, consisting of drillpipes and of the bottom hole assembly, is regarded as a torsional pendulum described by a lumped-parameter model with one or multiple degrees of freedom (DOF).

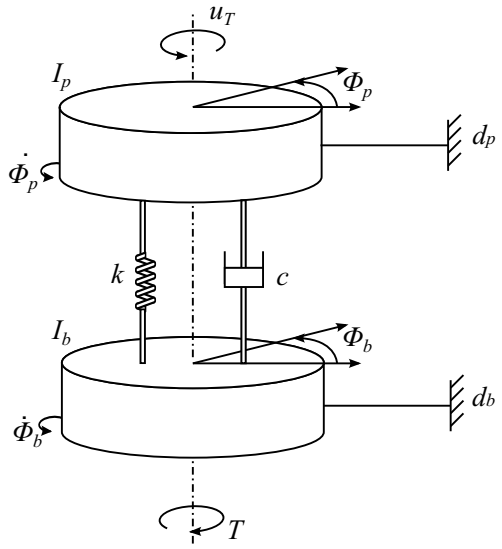

Figure 2: Lumped parameter model of a rotary drilling rig.

Figure 2 shows the simplified two-degree-of-freedom torsional model of a

conventional vertical drillstring proposed in [57]. The inertial masses I_p and I_b, locally damped by d_p and d_b, are connected one to each other by a linear spring with torsional stiffness k and torsional damping c. The equations of motion can be represented as follows:

$$\begin{cases} I_p\ddot{\Phi}_p + c\left(\dot{\Phi}_p - \dot{\Phi}_b\right) + k\left(\Phi_p - \Phi_b\right) + d_p\dot{\Phi}_p = u_T, \\ I_b\ddot{\Phi}_b - c\left(\dot{\Phi}_p - \dot{\Phi}_b\right) - k\left(\Phi_p - \Phi_b\right) + d_b\dot{\Phi}_b = -T(\dot{\Phi}_b), \end{cases} \tag{1}$$

where Φ_p and Φ_b are the angular displacements of the rotary table and of the BHA respectively. The control signal u_T is the drive torque coming from the rotary table transmission box used to regulate the rotary angular velocity $\dot{\Phi}_b$. The frictional torque T represents the torque on bit and the nonlinear frictional forces along the drill collars.

2.1.2. Axial dynamics

A simplified model described by an ordinary differential equation is presented in [16]; the modeling strategy is inspired by the fact that any mass subject to a force in stable equilibrium acts as a harmonic oscillator for small vibrations. More precisely, the damped harmonic oscillator model describing the longitudinal drillstring motion is:

$$m_0\ddot{\nu} + c_0\left(\dot{\nu} + \rho(t)\right) + k_0\nu = -\mu_1 T(\dot{\Phi}_b), \tag{2}$$

where the variable ν is defined as: $\nu = U_b - \rho_0 t$.

Notations m_0, c_0, and k_0 represent the mass, damping and spring constants; U_b, $\dot{U}_b$ and $\ddot{U}_b$ denote the bottom hole axial variables: position, velocity and acceleration, respectively. The coefficient μ_1 is given by the following relation [22]:

$$\mu_1 = 2\left(R_b\mu_{bit}c_{bit}\right)^{-1},$$

where R_b is the bit radius, μ_{bit} is the friction coefficient at the bit-rock contact, and c_{bit} is the so-called bit coefficient. For a bladed bit, c_{bit} is equal to the dimensionless length of the cutting edge (and independent of the number of

blades). For a flat bit, c_{bit} is computed as follows:

$$c_{bit} = \frac{6 + 4\rho_{bit}}{6 + 3\rho_{bit}}, \tag{3}$$

where ρ_{bit} is the radial rate of increase of cutter density. Notice that in (3), c_{bit} varies between 1 and 4/3 and may be considered as a constant.

The system is controlled through the rate of penetration $\rho(t)$, which is an axial speed imposed at the surface, ρ_0 is a constant nominal value. The torque on bit function T depending on the bit angular velocity couples the axial model with the torsional one.

2.1.3. Torsional-axial dynamics

A lumped parameter model that takes into consideration the axial and torsional vibration modes of a rotary drilling system is studied in [34], [35], [62]. Figure 3 shows the physical model as a two degrees-of-freedom system (one-axial and one-torsional) to describe the axial and torsional vibrations of the drillstring. The torsional part of the model idealizes the drillstring as a torsional pendulum, and the axial part of the model idealizes the BHA and the drillstring as a lumped mass M.

The governing equations of motion are given by:

$$\begin{cases} I\dfrac{d^2\Phi_b}{dt^2} + k(\Phi_b - \Phi_{b0}) = T_0 - T \\ M\dfrac{d^2U_b}{dt^2} = W_0 - W, \end{cases} \tag{4}$$

where the variables U_b and Φ_b stand for the vertical and angular positions of the bit, respectively. The mechanical elements representing the BHA are: M, the point mass; I, the moment of inertia; and k, the spring stiffness representing the torsional rigidity of the drill pipe. The torque and the weight on bit are denoted by T and W respectively. The stationary variables Φ_{b0}, T_0 and W_0, associated with the trivial solution of (4), satisfy:

$$\begin{aligned} \Phi_{b0} &= \Omega_0 t - \frac{T_0}{k}, \\ W_0 &= W_s - H_0 \end{aligned}$$

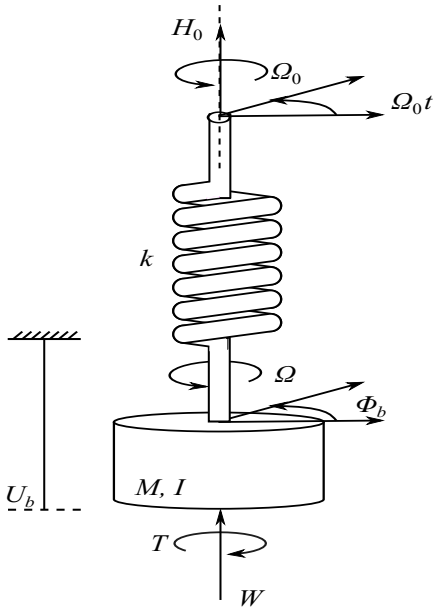

Figure 3: Simplified model of the drilling system proposed in [62].

where Ω_0 is a prescribed angular velocity, H_0 is a constant upward tension and W_s is the submerged weight of the drillstring.

A shortcoming of model (4) is that the dissipation in axial and torsional components is omitted, which may be quite unrealistic. Furthermore, the axial compliance of the drillpipes is not considered.

Some of these deficiencies were accounted in the model proposed in [6], given by:

$$\begin{cases} I\dfrac{d^2\Phi_b}{dt^2} + k_t(\Phi_b - \Omega_0 t) = T_0 - T \\ M\dfrac{d^2U_b}{dt^2} + d\dfrac{dU_b}{dt} + k_a\left(U_b - \rho_0 t\right) = W_0 - W, \end{cases} \tag{5}$$

where k_t, k_a denote the torsional and axial spring stiffness and the friction parameter d characterizes viscous friction along the BHA.

An improved version of the lumped parameter model describing the coupled torsional-axial drilling dynamics is proposed in [55]. The suggested governing

equations are given by:

$$\begin{cases} I\dfrac{d^2\Phi_b}{dt^2} + d_t\dfrac{d\Phi_b}{dt} + k_t(\Phi_b - \Omega_0 t) = T_0 - T \\ M\dfrac{d^2U_b}{dt^2} + d_a\dfrac{dU_b}{dt} + k_a\left(U_b - \rho_0 t\right) = W_0 - W, \end{cases} \tag{6}$$

where d_t and d_a represent the viscous damping coefficients accounting for dissipation in the torsional and axial directions, respectively.

Model (6) is used for developing a local stability analysis to determine the stable and unstable operating regimes in the weight on bit-rotary speed parameter plane yielding some operating guidelines for practical purposes [55].

2.2. Distributed parameter model: wave equation

To the best of the authors' knowledge, the very first model of drilling vibrations was developed in the sixties at the Shell Development Company, by J.J. Bailey [4] and I. Finnie [31]. They proposed a wave equation model to analytically treat the longitudinal and torsional drilling vibrations. Due to the accuracy of this modeling approach in reproducing the drilling behavior, regarding its distributed nature, it constitutes the basis of several recent contributions on drilling analysis and control.

The axial and angular drillstring dynamics can be derived by considering elastic deformations and using continuity equations and state and momentum balance of the pipe dynamics [24], [37]. The equation describing the traveling waves in a flexible rod can be derived from the *fundamental elasticity law* which establishes a relation between the local relative compression (strain) and the infinitesimal tension applied at a given point, see for instance [7], [25].

Consider the drillstring as a flexible rod of length L. Denoting the axial displacement by $U(s,t)$ and the strain by $h(s,t) = (U(s,t) - U(s+ds,t))/ds$, where $(s,t) \in [0,L] \times [0,\infty)$, the axial motion is described by [2]:

$$\frac{\partial h}{\partial t}(s,t) + \frac{\partial}{\partial s}\left(\frac{\partial U}{\partial t}(s,t)\right) = 0, \tag{7}$$

and, according to the *fundamental principle of dynamics*:

$$\rho_a\frac{\partial^2 U}{\partial t^2}(s,t) + E\frac{\partial h}{\partial s}(s,t) = -\gamma_a E\frac{\partial U}{\partial t}(s,t) \tag{8}$$

where ρ_a is the pipe mass density, E is Young's modulus and γ_a is a damping constant representing the shear stresses between the pipe and mud.

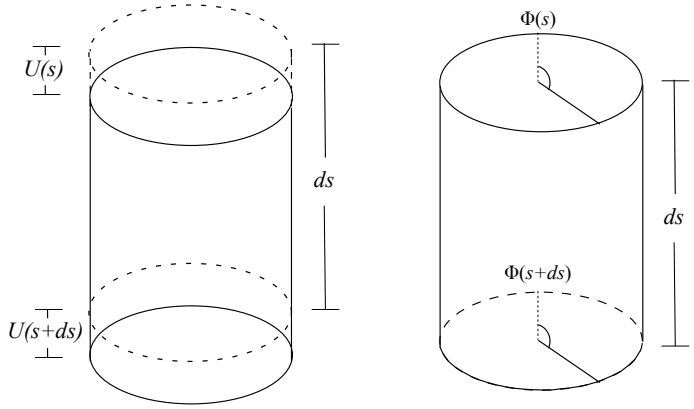

Figure 4: Infinitesimal rod element.

Similarly, for the angular motion, denote the angular displacement as $\Phi(s,t)$ and the shear strain (given as twist per unit length) as $f(s,t) = (\Phi(s,t) - \Phi(s+ds,t))/ds$, see Figure 4, the equations for the angular motion are:

$$\frac{\partial f}{\partial t}(s,t) + \frac{\partial}{\partial s}\left(\frac{\partial \Phi}{\partial t}(s,t)\right) = 0 \tag{9}$$

$$\rho_a \frac{\partial^2 \Phi}{\partial t^2}(s,t) + G\frac{\partial f}{\partial s}(s,t) = -\gamma_t G \frac{\partial \Phi}{\partial t}(s,t) \tag{10}$$

where G is the shear modulus and γ_t is a damping constant representing the shear stresses between the pipe and mud.

Combining equations (7) and (8) and, respectively, (9) and (10), we get two 1-dimensional wave equations:

$$\frac{\partial^2 U}{\partial t^2}(s,t) = c_a^2 \frac{\partial^2 U}{\partial s^2}(s,t) - \gamma_a \frac{\partial U}{\partial t}(s,t), \qquad s \in (0,L), \tag{11}$$

$$\frac{\partial^2 \Phi}{\partial t^2}(s,t) = c_t^2 \frac{\partial^2 \Phi}{\partial s^2}(s,t) - \gamma_t \frac{\partial \Phi}{\partial t}(s,t), \qquad s \in (0,L), \tag{12}$$

The propagation speeds of the torsional and axial waves c_a, c_t can be computed as:

$$c_a = \sqrt{\frac{E}{\rho_a}} \quad \text{and} \quad c_t = \sqrt{\frac{G}{\rho_a}}. \tag{13}$$

Some authors refer that the distributed damping may be considered negligible since most of the energy dissipation in is taking place at the bit-rock interface, see for example [1], [5], [11], [63], [72]. Although neglecting damping simplifies the system analysis, it may jeopardize the complete understanding of the drilling dynamics [2], [17]. Under the assumption that γ_t and γ_a are null, the coupled torsional-axial excitations of a drillstring of length L, described by the rotary angle $\Phi(s,t)$ and the longitudinal position $U(s,t)$ can be modeled by the undamped wave equations:

$$\frac{\partial^2 \Phi}{\partial t^2}(s,t) = c_t^2 \frac{\partial^2 \Phi}{\partial s^2}(s,t), \tag{14}$$

$$\frac{\partial^2 U}{\partial t^2}(s,t) = c_a^2 \frac{\partial^2 U}{\partial s^2}(s,t), \tag{15}$$

Infinite dimensional models can be approximated by finite dimensional systems (see for instance [27]). Conceptually this can be viewed as choosing a finite $ds > 0$ for the drill string elements shown in Figure 4 [2]. This kind of model is often understood as the continuum model broken up into a series of mass-spring-damper systems representing lumped inertia, stiffness and damping. In [2] is shown that the lumped models can be obtained by the same approach as the distributed ones but using finite non-zero segments; a comparison between lumped parameter models with different number of lumped inertias and the exact distributed system is provided.

2.2.1. Boundary conditions

It is well known that torsional vibrations contribute to the excitation of axial oscillations, i.e., the high bit speed level provoked by the stick-slip phenomenon can excite severe axial vibrations in the bottom hole assembly which may cause bit-bounce, excessive bit wear and reduction in the penetration rate [46], [68], [78]. These self-excited oscillations are intimately coupled and may occur simultaneously [18], [75], [77].

In general, although the wave equations describing the drilling system dynamics are uncoupled in the domain, the coupling of the torsional and axial

dynamics is represented through the bit-rock interaction law at the boundary. An appropriate choice of boundary conditions allows characterizing the propagating waves along the drillstring. Several equations have been proposed to describe the axial and torsional dynamics taking place at the upper and lower ends of the drillstring; some of them are reviewed in this section.

In the sequel the spatial variable is chosen such that $s = 0$ denotes the top of the drillstring and $s = L$ its bottom. The following set of boundary conditions considers that there exist a mismatch between the boundary torque u_T and the rotational speed of the load $\frac{\partial \Phi}{\partial t}(0,t)$ and between the boundary force u_H and the axial sped of the load $\frac{\partial U}{\partial t}(0,t)$ [8], [65]. The boundary conditions corresponding to the torsional dynamics are:

$$GJ\frac{\partial \Phi}{\partial s}(0,t) = \beta\frac{\partial \Phi}{\partial t}(0,t) - u_T(t) \tag{16a}$$

$$GJ\frac{\partial \Phi}{\partial s}(L,t) = -I_B\frac{\partial^2 \Phi}{\partial t^2}(L,t) - T\left(\frac{\partial \Phi}{\partial t}(L,t)\right), \tag{16b}$$

and for the axial dynamics, the boundary conditions are given by:

$$E\Gamma\frac{\partial U}{\partial s}(0,t) = \alpha\frac{\partial U}{\partial t}(0,t) - u_H(t) \tag{17a}$$

$$E\Gamma\frac{\partial U}{\partial s}(L,t) = -M_B\frac{\partial^2 U}{\partial t^2}(L,t) - T\left(\frac{\partial \Phi}{\partial t}(L,t)\right). \tag{17b}$$

In the boundary condition (16a), u_T represents the torque produced by the rotary table motor and $\beta\partial\Phi/\partial t(0,t) - u_T(t)$ designates the difference between the motor speed and rotational speed of the first pipe (where β denotes the angular momentum at the top extremity). In (17a), u_H is the brake motor control (upward hook force) and $\alpha\partial U/\partial t(0,t)$ represents a friction force of viscous type (where α is the viscous friction coefficient). It is assumed that the drilling system can be controlled by the boundary force u_H and the boundary torque u_T.

Some of geometrical parameters of the drillstring model that are assumed to be spatially and timely constant are: the drillstring's cross-section Γ, its second moment of area J, the mass M_B and the inertia moment[1] of the drill bit I_B.

[1]The inertia moment is such that $I_B = M_B\, r^2$, where r is the averaged radius of drillpipe.

The function T (representing the coupling mechanism between torsional and axial vibration modes) considered in the bottom boundary conditions accounts for the frictional torque resulting from the interaction between the drill bit and the rock. The modeling of the torque on the bit constitutes a crucial aspect of the system description since it allows to reproduce the vibrational phenomena; this subject will be discussed in Section 3.

A different top boundary condition is proposed in [16], here it is assumed that the speed at the surface is restricted to a constant value Ω:

$$\Phi(0,t) = \Omega t, \tag{18}$$

This boundary condition is only a pure kinematic description of the drillstring upper part.

The following equation constitutes an alternative top boundary condition inspired by the Newton's second law of motion, see for instance [19]:

$$I_T \frac{\partial^2 \Phi}{\partial t^2}(0,t) = -T_T(t) + u_T(t).$$

The effective moment of inertia of the top-drive is denoted by I_T, and the function $T_T(t)$, describing the transmitted torque and damping due to viscous effects, is given by:

$$T_T(t) = -GJ\frac{\partial \Phi}{\partial s}(0,t) + \beta \frac{\partial \Phi}{\partial t}(0,t).$$

Different boundary conditions at the bottom end can be derived from the analysis developed in [22] about the characterization of the cutting and friction elements of the torque and of the weight on bit when a drag-type bit[2] is considered. In the modeling of the frictional interface for a drag bit, is convenient to characterize the action of rock cutting by individual cutters instead of assuming the rock-bit interface as an equivalent frictional contact. Under this assumption, a relation between the weight on bit W, the torque on bit T and the states must be established (see Section 3.7).

[2] A drag bit is a specific type of cutting device consisting of n identical blades symmetrically distributed around the axis of revolution.

Consider the set of boundary conditions:

$$\Gamma \frac{\partial^2 U}{\partial t^2}(L,t) = -E\Gamma \frac{\partial U}{\partial s}(L,t) - W \tag{19}$$

$$J \frac{\partial^2 \Phi}{\partial t^2}(L,t) = -GJ \frac{\partial \Phi}{\partial s}(L,t) - T \tag{20}$$

where Γ, J are the area and polar inertia of the lowermost section of the drillstring. Introducing the relations presented in Section 3.7 (see Equations (54), (55)), the boundary conditions (19)-(20) can be rewritten as:

$$\Gamma \frac{\partial^2 U}{\partial t^2}(L,t) = -R_b \upsilon \epsilon n \left[U(L,t) - U(L,t-t_n)\right] - W_f - E\Gamma \frac{\partial U}{\partial s}(L,t) \tag{21}$$

$$J \frac{\partial^2 \Phi}{\partial t^2}(L,t) = -\frac{1}{2} R_b^2 \epsilon n \left[U(L,t) - U(L,t-t_n)\right] - T_f - GJ \frac{\partial \Phi}{\partial s}(L,t). \tag{22}$$

where R_b is the bit radius, the constant υ characterizes the cutting force orientation, ϵ is the intrinsic specific energy and W_f, T_f are the frictional components of the weight on bit and torque. The state-dependent time delay t_n is implicitly defined in (53) [41].

At the topside, can be assumed that the torque and weight on the drillstring are imposed by the drilling operator, then the top boundary condition is given by:

$$E\Gamma \frac{\partial U}{\partial s}(0,t) = W_{op}(t) \quad GJ \frac{\partial \Phi}{\partial s}(0,t) = T_{op}(t), \tag{23}$$

2.3. Neutral-type time-delay models

The wave equation model provides a realistic description of the distributed system variables; however, under certain circumstances, it is convenient to deal with a relatively simpler model involving just the primary interest variables. It will be shown that it is possible to derive, from the wave equations, equivalent input-output models described by neutral-type time-delay equations relating the variables at both ends of the drilling rod.

Integration along characteristics of the hyperbolic PDE allows the association of a certain system of functional differential equations to the mixed problem, more precisely, a one-to-one correspondence may be established and proved between the solutions of the mixed problem for hyperbolic PDE and the initial

value problem for the associated system of functional equations [60]. By reducing a boundary value problem to a neutral-type time-delay equation we are able to exploit techniques from delay systems theory to gain insight into the complexity involved in the analysis and simulation of PDE models.

The *method of d'Alembert* provides a solution to the one-dimensional wave equation. Introducing the variables $\gamma = t + s/c_t$ and $\eta = t - s/c_t$, the general solution of the undamped wave equation (14), describing the torsional drilling behavior, is given by:

$$\Phi(s,t) = \phi(\gamma) + \psi(\eta), \tag{24}$$

where ϕ and ψ are arbitrary continuously differentiable real-valued functions, with ϕ representing an arbitrary up-traveling wave and ψ an arbitrary down-traveling wave.

Let $\dot{\Phi}_b(t)$ be the angular velocity at the bottom extremity of the rod:

$$\dot{\Phi}_b(t) = \frac{\partial \Phi}{\partial t}(L,t) = \dot{\phi}(t+\tau) + \dot{\psi}(t-\tau). \tag{25}$$

After some simple mathematical manipulations based on the substitution of (24) into the boundary conditions (16), we get a torsional drilling model described by the neutral-type time-delay equation:

$$\begin{aligned} \ddot{\Phi}_b(t) - \Upsilon\ddot{\Phi}_b(t-2\tau) &= -\Psi\dot{\Phi}_b(t) - \Upsilon\Psi\dot{\Phi}_b(t-2\tau) - \frac{1}{I_B}T\Big(\dot{\Phi}_b(t)\Big) \\ &\quad + \frac{1}{I_B}\Upsilon T\Big(\dot{\Phi}_b(t-2\tau)\Big) + \Pi_\Omega u_T(t-\tau), \end{aligned} \tag{26}$$

where

$$\Pi_\Omega = \frac{2\Psi}{\beta + \tilde{c}GJ}, \quad \Upsilon = \frac{\beta - \tilde{c}GJ}{\beta + \tilde{c}GJ}, \quad \Psi = \frac{\tilde{c}GJ}{I_B}, \quad \tau = L/c_t. \tag{27}$$

Similarly, the wave equation (15) with boundary conditions (17), corresponding to the axial drilling dynamics is transformed into the following neutral-type equation:

$$\begin{aligned} \ddot{U}_b(t) - \tilde{\Upsilon}\ddot{U}_b(t-2\tilde{\tau}) &= -\tilde{\Psi}\dot{U}_b(t) - \tilde{\Upsilon}\tilde{\Psi}\dot{U}_b(t-2\tilde{\tau}) - \frac{1}{M_B}T\Big(\dot{\Phi}_b(t)\Big) \\ &\quad + \frac{1}{M_B}\tilde{\Upsilon}T\Big(\dot{\Phi}_b(t-2\tilde{\tau})\Big) + \tilde{\Pi}_\rho u_H(t-\tilde{\tau}), \end{aligned} \tag{28}$$

where $\dot{U}_b(t)$ is the axial velocity at the bottom extremity, and

$$\tilde{\Pi}_\rho = \frac{2\tilde{\Psi}}{\alpha + cE\Gamma}, \quad \tilde{\Upsilon} = \frac{\alpha - cE\Gamma}{\alpha + cE\Gamma}, \quad \tilde{\Psi} = \frac{cE\Gamma}{M_B}, \quad \tilde{\tau} = L/c_a. \tag{29}$$

It is important to point out that the delays τ and $\tilde{\tau}$ represent the time that the torsional and the axial waves take to travel from one to the other extremity of the drillstring; notice that they are inversely proportional to the wave propagation speeds c_t, c_a.

2.4. Coupled PDE-ODE models

Some manipulations of the drilling models have been proposed to facilitate the design of control laws to eliminate drilling vibrations. For example, in [12] and in [13], torsional drilling vibrations are represented as the cascade of two transport PDEs coupled to an ODE. The model is derived from the undamped wave equation with the following normalized boundary conditions (see Section 2.2):

$$\begin{cases} \dfrac{\partial^2 \Phi}{\partial t^2}(s,t) = \dfrac{\partial^2 \Phi}{\partial s^2}(s,t) \\ \dfrac{\partial \Phi}{\partial s}(0,t) = u_T(t) \\ \dfrac{\partial^2 \Phi}{\partial t^2}(1,t) = aF\left(\dfrac{\partial \Phi}{\partial t}(1,t)\right) + a\dfrac{\partial \Phi}{\partial s}(1,t) \end{cases} \tag{30}$$

where the constant a is positive and F is a given nonlinear function representing the rock on bit friction which is considered to be highly uncertain. Notice that this model consists in a wave PDE in one dimension with actuation on one boundary and with an unknown anti-damping term on the opposite boundary.

The derived PDE-ODE model is constructed under the assumption that the control objective is to stabilize the angular velocity $\frac{\partial \Phi}{\partial t}(\cdot, t)$ toward a given uniform rotatory speed $\frac{\partial \Phi^r}{\partial t}$. After a linearization of (30), we obtain:

$$\begin{cases} \dfrac{\partial^2 \Phi}{\partial t^2}(s,t) = \dfrac{\partial^2 \Phi}{\partial s^2}(s,t) \\ \dfrac{\partial \Phi}{\partial s}(0,t) = u_T(t) \\ \dfrac{\partial^2 \Phi}{\partial t^2}(1,t) = aq\dfrac{\partial \Phi}{\partial t}(1,t) + a\left[\dfrac{\partial \Phi}{\partial s}(1,t) - g\right] \end{cases} \tag{31}$$

where the anti-damping parameter $q = \frac{dF(\frac{\partial \Phi^r}{\partial t})}{d(\frac{\partial \Phi}{\partial t})} > 0$ and the trajectory coefficient $g = -F\left(\frac{\partial \Phi^r}{\partial t}\right)$ are unknown. System (31) can be reformulated by introducing the following intermediate Riemann variables and transformed control variable:

$$\lambda(s,t) = \frac{\partial \Phi}{\partial t}(s,t) + \frac{\partial \Phi}{\partial s}(s,t) - \hat{g}(t)$$
$$\omega(s,t) = \frac{\partial \Phi}{\partial t}(s,t) - \frac{\partial \Phi}{\partial s}(s,t) + \hat{g}(t)$$
$$V(t) = \frac{\partial \Phi}{\partial t}(0,t) + u_T(T) - \hat{g}(t).$$

The obtained system with the estimation error $\tilde{g}(t) = g(t) - \hat{g}(t)$ can be written as:

$$\frac{\partial^2 \Phi}{\partial t^2}(1,t) = a(q-1)\frac{\partial \Phi}{\partial t}(1,t) + a\left[\lambda(1,t) - \tilde{g}(t)\right] \tag{32}$$
$$\frac{\partial \lambda}{\partial t}(s,t) = \frac{\partial \lambda}{\partial s}(s,t) - \dot{\hat{g}}(t) \tag{33}$$
$$\lambda(0,t) = V(t) \tag{34}$$
$$\frac{\partial \omega}{\partial t}(s,t) = -\frac{\partial \omega}{\partial s}(s,t) + \dot{\hat{g}}(t) \tag{35}$$
$$\omega(1,t) = 2\frac{\partial \Phi}{\partial t}(1,t) - \lambda(1,t). \tag{36}$$

In this new framework, the wave phenomenon is represented as the cascade of two transport PDEs with source term, with one ODE being driven by the first of the two PDEs. The ODE (32) with state $\frac{\partial \Phi}{\partial t}(1,\cdot)$ plays a central role and it has to be stabilized through the transport equation (33) controlled at the boundary $s = 0$. A second transport phenomenon (35) with similar source term is also present, in the opposite direction, accounting for the reflection of the wave at $s = 1$ [12].

A different model transformation for the wave equation describing torsional drilling vibrations is proposed in [63]. The model simplification is based on a

system of the form (30), but without neglecting the distributed viscous damping:

$$\begin{cases} \dfrac{\partial^2\Phi}{\partial t^2}(s,t) = \dfrac{\partial^2\Phi}{\partial s^2}(s,t) - \gamma_t \dfrac{\partial\Phi}{\partial t}(s,t) \\ \dfrac{\partial\Phi}{\partial s}(0,t) = u_T(t) \\ \dfrac{\partial^2\Phi}{\partial t^2}(1,t) = aF\left(\dfrac{\partial\Phi}{\partial t}(1,t)\right) + a\dfrac{\partial\Phi}{\partial s}(1,t) \end{cases} \tag{37}$$

The trajectories of (37) corresponding to a uniform constant rotary speed $\frac{\partial\Phi^r}{\partial t}(s,t)$ are of the form:

$$\Phi^r(s,t) = \frac{\gamma_t}{2}\frac{\partial\Phi^r}{\partial t}s^2 - F\left(\frac{\partial\Phi^r}{\partial t}\right)s + \frac{\partial\Phi^r}{\partial t}t + \Phi_0 \tag{38}$$

with the following reference input:

$$\bar{u}_T = \gamma_t\frac{\partial\Phi^r}{\partial t} - F\left(\frac{\partial\Phi^r}{\partial t}\right) \tag{39}$$

Linearizing the second boundary condition of (37) around a reference trajectory of the form (38)-(39) for a given reference velocity $\frac{\partial\Phi^r}{\partial t}$, while keeping the in-domain damping and the drill bit inertia terms, we obtain:

$$\begin{cases} \dfrac{\partial^2\Phi}{\partial t^2}(s,t) = \dfrac{\partial^2\Phi}{\partial s^2}(s,t) - \gamma_t \dfrac{\partial\Phi}{\partial t}(s,t) \\ \dfrac{\partial\Phi}{\partial s}(0,t) = u_T(t) \\ \dfrac{\partial^2\Phi}{\partial t^2}(1,t) = aq\dfrac{\partial\Phi}{\partial t}(1,t) + a\dfrac{\partial\Phi}{\partial s}(1,t) \end{cases} \tag{40}$$

Defining the following set of state variables:

$$\bar{\Phi}(s,t) = \frac{\partial(\Phi-\Phi^r)}{\partial s}(s,t), \quad \Phi_b = \frac{\partial\Phi}{\partial t}(1,t), \quad \bar{u}_T = u_T - u_T^r,$$

yields the following coupled PDE-ODE system:

$$\frac{\partial^2\bar{\Phi}}{\partial t^2}(s,t) = \frac{\partial^2\bar{\Phi}}{\partial s^2}(s,t) - \gamma\frac{\partial\bar{\Phi}}{\partial t}(s,t) \tag{41}$$

$$\bar{\Phi}(0,t) = \bar{u}_T \tag{42}$$

$$\frac{\partial\bar{\Phi}}{\partial s}(1,t) = a\bar{\Phi}(1,t) + (\gamma+aq)\Phi_b(t) \tag{43}$$

$$\dot{\Phi}_b(t) = aq\Phi_b(t) + a\bar{\Phi}(1,t). \tag{44}$$

This modeling approach allows the design of an exponential stabilizing controller based on backstepping techniques; details can be found in [63].

Models given in (32)-(36) and in (41)-(44) describe the torsional behavior of the drilling rod, neglecting their axial dynamics; a PDE-ODE model reproducing the coupled torsional-axial drilling vibrations is presented in [24]. The proposed model is derived form the damped wave equations given in (11) and in (12) subject to boundary conditions reflecting the action of rock cutting by individual cutters (see Equations (19)-(22)).

To develop the transformation, the following variables are defined:

$$U_1 = \frac{\partial U}{\partial t} - c_t \frac{\partial U}{\partial s}, \qquad U_2 = \frac{\partial U}{\partial t} + c_t \frac{\partial U}{\partial s}$$
$$\Phi_1 = \frac{\partial \Phi}{\partial t} - c_a \frac{\partial \Phi}{\partial s}, \qquad \Phi_2 = \frac{\partial \Phi}{\partial t} + c_a \frac{\partial \Phi}{\partial s}$$

Denoting $X = U(L,t)$, $Z = \Phi(L,t)$, we obtain the following system of transport PDEs coupled with a delay differential equation:

$$\begin{aligned}
\frac{\partial U_1}{\partial t} + c_a \frac{\partial U_1}{\partial s} &= -\gamma_a (U_1 + U_2)/2 \\
\frac{\partial U_2}{\partial t} - c_a \frac{\partial U_2}{\partial s} &= -\gamma_a (U_1 + U_2)/2 \\
\frac{\partial \Phi_1}{\partial t} + c_t \frac{\partial \Phi_1}{\partial s} &= -\gamma_t (\Phi_1 + \Phi_2)/2 \\
\frac{\partial \Phi_2}{\partial t} - c_t \frac{\partial \Phi_2}{\partial s} &= -\gamma_t (\Phi_1 + \Phi_2)/2 \\
U_1(0,t) &= u_H(t) \\
\Phi_1(0,t) &= u_T(t) \\
U_2(L,t) &= -U_1(L,t) + 2\dot{X}(t) \\
\Phi_2(L,t) &= -\Phi_1(L,t) + 2\dot{Z}(t)
\end{aligned}$$

$$\ddot{X}(t) = -c_1[X(t) - X(t-t_n)] - c_2\dot{X}(t) + c_3 U_1(L,t)$$
$$\ddot{Z}(t) = -c_1'[X(t) - X(t-t_n)] - c_2'\dot{Z}(t) + c_3' \Phi_2(L,t)$$

where u_H and u_T are the control inputs and the parameters c_1, c_1', c_2, c_2', c_3, c_3' are deduced from the boundary conditions (21), (22).

2.5. Remarks and related literature

The complexity of the drilling dynamics makes unreasonable the construction of a model with worldwide acceptability. Several approaches to describe the mechanisms triggering drillstring vibration have been proposed; drilling models can be established either in the frequency [29], [38] or the time domain [46], [18].

Four general categories of time-domain drillstring models can be distinguished: distributed parameter models, lumped parameter models, time-delay models and coupled PDE-ODE models, being the first ones those arising in a more natural way. The distributed parameter models corresponding to the 1-dimensional wave equation describe the propagating waves traveling from the bottom to the top of the drillstring. These models are usually approximated by a series of lumped mass-spring damper systems, where the case of using a single degree of freedom lumped mass is the most common but the multi-degree of freedom approximations have been proposed as well. Reduced models are preferred because of their simplicity regarding the stability analysis and control design, however, they don't capture all the system dynamics and their accuracy is reduced even for higher-order models. Infinite dimensional models are closer to represent the real behavior of the drillstring. Neutral-type time-delay models and coupled PDE-ODE models are obtained through direct transformations of the distributed parameter models, they are accurate in reproducing the drillstring vibrations and reduce the complexity involved in the stability analysis and control design. Table 1 summarizes the attributes and shortcomings of these modeling approaches.

Table 1: Benefits and drawbacks of the drillstring models.

Model	**Advantages**	**Disadvantajes**
Lumped parameter	Describes the system dynamics in a simple way. Eases the basic understanding of the drilling dynamics. Simplifies the analysis and control design.	Disregards the distributed nature of the system. Involves important simplifications. Its accuracy depends on the involved DOF number.
Distributed parameter	Its derivation is natural regarding the distributed character of the system. Provides high accuracy in reproducing the rod oscillatory behavior.	Its accuracy depends on an appropriate choice of boundary conditions. The analysis may be complex under certain boundary conditions.
Neutral-type time-delay	Facilitates the system analysis. Eases the control design regarding the existing extensive literature for the stabilization of delay-systems.	Disregards the distributed nature of the system. For its derivation, the damping along the structure must be neglected. Its accuracy depends on the boundary conditions choice.
Coupled PDE-ODE	Provides high accuracy in reproducing the drilling dynamics. Eases the design of determined control strategies.	Hinders the understanding of the system oscillatory behavior. Its structure is useful only for the design of specific control strategies.

To choose a suitable modeling approach, it is essential to take into account the pursued research objective. Table 2 presents some of the references devoted to the study of the effects of the parameters variation on drillstring vibration, the stability analysis of the drilling dynamics and the control design to suppress undesirable behavior. All the studies were carried out based on a convenient modeling approach allowing the achievement of determined purposes.

Table 2: Drilling models and research objectives

Model	**Related literature**
Lumped parameter	In [39] a one DOF model is used to design a control strategy allowing a smooth bit rotation to reduce axial and lateral drilling vibrations. In [14] a two DOF lumped parameter model is used to analyze torsional vibrations when drilling with a polycrystalline diamond compact (PDC) bit. In [50] a one DOF model is used to investigate the effects of viscous damping, rotary speed and natural frequency on the stick-slip phenomenon. In [42] and [70] a two DOF model is used to design control strategies (active damping and $\mathcal{H}_\infty$, respectively) to tackle torsional drilling oscillations. In [57] a two DOF model is used to study practical strategies to avoid stick-slip vibrations. In [56] the design of a sliding-mode control is based on a torsional model of four DOF. In [15] a two DOF model is used for the design of the D-OSKILL controlller to suppress torsional vibrations. In [49] different reduced-order models describing radial, bending, and torsional motions of a drillstring system are developed; qualitative comparisons between models are made with experimental studies. In [51] a model of eight DOF is proposed to study the dynamic behavior of a drillstring subject to axial, torsional and lateral vibrations.
Distributed parameter	In [4] the very first analytic studies on torsional vibrations carried out; a wave equation model was considered. In [1] a distributed model was used to understand the vibrational phenomena within the framework of linear elastic theory. In [72] the undamped wave equation constitutes the basis for the design of a control mechanism designed to avoid the excitation of torsional oscillations. In [16] a distributed parameter model is used to investigate the drilling system stability through the direct method of Lyapounov.

	In [63] a flatness-based controller to suppress torsional oscillations are derived from a PDE model. In [11] an adaptive output-feedback controller for a wave PDE in one dimension model with actuation on one boundary and with an unknown anti-damping term on the opposite boundary was developed to treat the stick-slip instability. In [2] a distributed model and a linearized bit-rock interaction law is used to derive a graphical condition for the drilling stability based on the Nyquist stability criterion.
Neutral-type time-delay	In [5] the numerical solution of a neutral differential delay equation describing torsional waves on a driven drill-string under parametric variation is studied. In [9] a pair of coupled neutral-type time delay equations are used to describe axial and torsional vibrations. A pair of stabilizing controllers are designed based on a simplified model derived from the center manifold theorem and normal forms theory. In [65], a pair of delay differential equations are used to describe the coupled axial-torsional drilling vibrations. Based on this model, a controller guaranteeing the elimination of the stick-slip and bit-bounce is developed. In [66] a neutral-type time-delay model describing the oscillatory behavior in the drilling system is used to design a stabilizing control law based on the attractive ellipsoid method. In [76] the practical stabilization of a nonlinear neutral type time delay system describing the stick-slip phenomenon in the drilling process is addressed within the framework of Lyapunov theory.
Coupled PDE-ODE	In [63] a stabilizing controller based on backstepping techniques to suppress torsional oscillations are derived from a PDE-ODE model. In [13] an adaptive output-feedback controller for a wave PDE describing torsional drill string torsional instabilities is developed. The proposed controller requires only the measurements of top-boundary values.

	In [24] a detailed view of the control problem of the stabilization of axial-torsional drillstring vibrations described by a system of transport PDEs coupled with a delay differential equation is presented.

A comparative review of methods of modeling and controlling torsional vibrations within a experimental framework can be found in [58]; the required information to develop a laboratory model to reproduce torsional vibrations is also provided.

Additional references on the different drillstring vibration modeling and suppression methods are presented in [36]; the challenges posed by the presence of modern drilling techniques such as deviated drilling and use of vibrating downhole tools are discussed.

An important aspect in reproducing the nonlinearities giving rise to drilling vibrations is the modeling of the frictional torque characterizing the rock-bit interface; the following section addresses this topic.

3. Modeling of the bit-rock interaction

It is usually assumed that the growth of instabilities eventually leading to stick-slip and bit-bounce oscillations arises from the friction model, which empirically captures the interaction between the cutting device and the rock. An appropriate model of friction allows gaining insight into vibrational drillstring phenomena thus characterizing the dynamic behavior at bit level and making possible the development of appropriate control strategies to tackle this problem.

In this section, a summary of the most popular models of friction due to the contact between the cutting device and the drilling surface is presented.

3.1. Velocity weakening law

In [16], the model:

$$T(\dot{U}_b, \dot{\Phi}_b) = \zeta \dot{U}_b \mathrm{e}^{-\bar{\alpha}\dot{\Phi}_b}$$

is chosen to represent the bit-rock interaction, $\dot{U}_b$, and $\dot{\Phi}_b$ stand for the axial and angular velocities at the bottom extremity and ζ denotes the ability of the rock to be cut.

3.2. Stiction plus Coulomb friction

In [42] and [70], the torque on the bit is modeled through the expression:

$$T(\dot{\Phi}_b(t)) = c_b\dot{\Phi}_b(t) + T_{fb}(\dot{\Phi}_b(t))$$

where c_b is the damping viscous coefficient at the bit level and T_{fb} is the classical Coulomb plus static friction (dry friction) model, that is,

$$T_{fb}(\dot{\Phi}_b(t)) = \begin{cases} (T_{sb} - T_{cb})\text{sgn}(\dot{\Phi}_b(t)) & \text{if } \dot{\Phi}_b(t) \neq 0 \\ \\ T_{sb} & \text{if } \dot{\Phi}_b(t) = 0 \end{cases} \tag{45}$$

with $T_{sb} = \mu_{sb}W_{ob}R_b$ and $T_{cb} = \mu_{cb}W_{ob}R_b$ the static and Coulomb friction torques, μ_{sb}, $\mu_{cb} \in (0, 1)$ the static and Coulomb friction coefficients, W_{ob} is the weight on the bit and R_b is the bit radius.

The use of this modeling strategy is explained in [70] as follows: the maximum torque T_{sb} clamping the bit to zero speed is substantially larger than the Coulomb friction T_{cb} experienced when the bit is rotating. If $\dot{\Phi}_b = 0$, the friction torque will adjust to the torque in the drillstring maintaining a static equilibrium of the bit (see, for instance Figure 5).

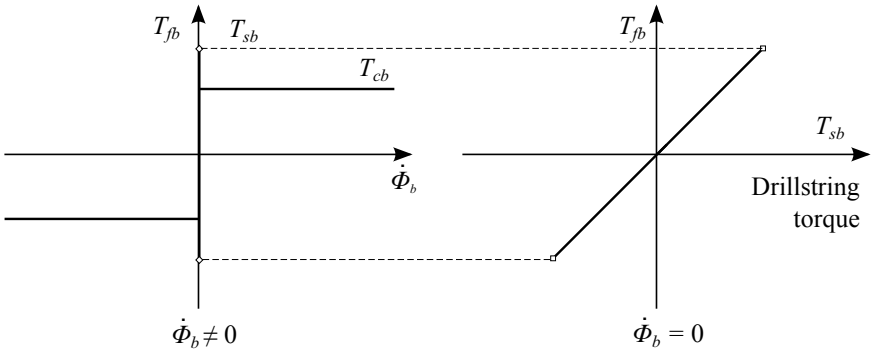

Figure 5: Coulomb and static friction.

3.3. Dry friction plus Karnopp's model

Another common model for $T_{f_b}(\dot{\Phi}_b(t))$ is defined below

$$T_{f_b}(\dot{\Phi}_b(t)) = \begin{cases} T_{eb} & \text{if } \left|\dot{\Phi}_b(t)\right| < D_v, \ \ |T_{eb}| \leq T_{sb} \\ & \text{(stick)} \\ T_{sb}\text{sgn}(T_{eb}) & \text{if } \left|\dot{\Phi}_b(t)\right| < D_v, \ \ |T_{eb}| > T_{sb} \\ & \text{(stick-to-slip transition)} \\ T_{cb}\text{sgn}(\dot{\Phi}_b(t)) & \text{if } \left|\dot{\Phi}_b(t)\right| \geq D_v, \\ & \text{(slip)} \end{cases}$$

where $D_v > 0$ specifies a small enough neighborhood of $\dot{\Phi}_b(t) = 0$ and T_{eb} is the applied external torque that must overcome the static friction torque T_{sb} to make the bit move. For a lumped parameter model of the form (1), T_{eb} is modeled as follows:

$$T_{eb} = c\left(\dot{\Phi}_p - \dot{\Phi}_b\right) + k\left(\Phi_p - \Phi_b\right) - c_b\dot{\Phi}_b. \tag{46}$$

For a PDE model such as the one stated in (15)-(16), the external torque T_{eb} can be described by:

$$T_{eb} = c\frac{\partial^2\Phi}{\partial t \partial x}(L,t) + k\frac{\partial\Phi}{\partial x}(L,t) - c_b\frac{\partial\Phi}{\partial t}(L,t). \tag{47}$$

This model combines the dry friction model (45) with the Karnopp's model proposed in [44] and introduces a zero velocity band (see Figure 6).

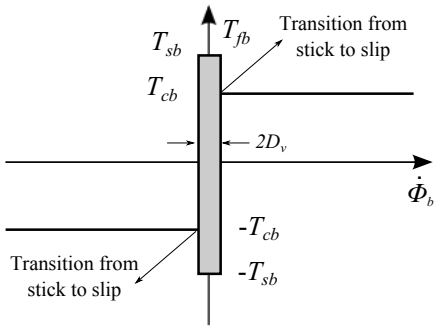

Figure 6: Dry friction plus Karnopp's model.

3.4. Karnopp's model with a decaying friction term

The function governing friction in the slip phase is chosen as a decaying function inspired by the experimental results given in [14]:

$$T_{f_b}(\dot{\Phi}_b(t)) = \begin{cases} \min\{|T_{eb}|, T_{sb}\}\mathrm{sgn}(T_{eb}) & \text{if } \left|\dot{\Phi}_b(t)\right| < D_v \\ \\ f_b(\dot{\Phi}_b(t))\mathrm{sgn}(\dot{\Phi}_b(t)) & \text{if } \left|\dot{\Phi}_b(t)\right| \geq D_v \end{cases} \tag{48}$$

where the external torque T_{eb} is defined in (46) for an ODE model, and in (47) for a PDE model. The function f_b has the following form:

$$f_b(\dot{\Phi}_b(t)) = W_{ob} R_b \mu_b(\dot{\Phi}_b(t)), \tag{49}$$

where the dry friction coefficient at the bit μ_b is given by:

$$\mu_b(\dot{\Phi}_b(t)) = \frac{\mu_{sb} - \mu_{cb}}{1 + \gamma_b \left|\dot{\Phi}_b(t)\right|} + \mu_{cb}, \tag{50}$$

constants μ_{cb} and μ_{sb} denote the Coulomb and static friction coefficients, and $0 < \gamma_b < 1$ is a constant defining the decaying velocity of T_{f_b} (see Figure 7). The static friction torque T_{sb} is given by $T_{sb} = \mu_{sb} W_{ob} R_b$.

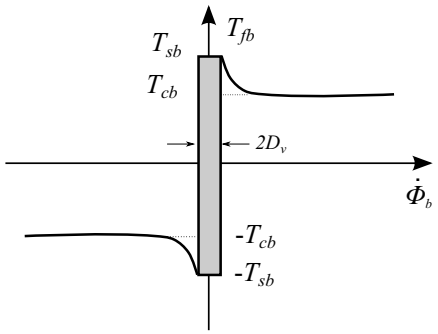

Figure 7: Karnopp's model with a decaying friction term.

3.5. Karnopp's model with an exponential decaying friction term

An alternative model for the torque on the bit defines an exponential decaying term in the slip phase [56]. It considers the expression given in (48) with $f_b(\dot{\Phi}_b(t))$ given in (49) but with the dry friction coefficient $\mu_b(\dot{\Phi}_b(t))$ defined as:

$$\mu_b(\dot{\Phi}_b(t)) \quad = \quad \mu_{cb} + (\mu_{sb} - \mu_{cb})\mathrm{e}^{-\gamma_b|\dot{\Phi}_b(t)|}. \tag{51}$$

Simulations results presented in [64] validate the proposed model.

3.6. Simplified torque on bit model

Is worth mentioning that the models presented above may be complicated for practical purposes. For this reason, the construction of a simplified model which captures their essential dynamic properties is of interest.

In [47] the following model is introduced:

$$T(\dot{\Phi}_b(t)) = \frac{2\bar{k}\dot{\Phi}_b(t)}{\dot{\Phi}_b^2(t) + \bar{k}^2} \tag{52}$$

where $\bar{k}$ is a positive parameter. This model is simpler than those presented above and effectively reproduces the behavior of the friction at the bit level (see Figure 8).

3.7. Frictional forces at the bit-rock interface considering individual cutters

In general, the modeling approaches to approximate the interaction between the cutting tool and the rock formation consider the bit-rock interface as an

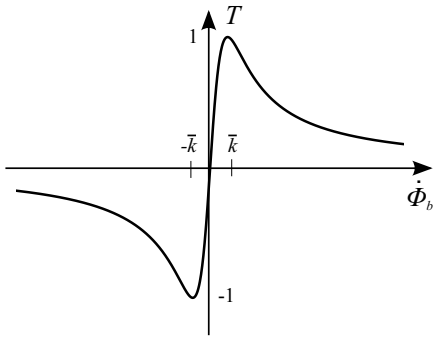

Figure 8: Simplified torque on bit model proposed in [47].

equivalent frictional contact, however, when considering a bit of drag-type[3], is convenient to characterize the action of rock cutting by individual cutters. This kind of bit-rock frictional interface is studied in [24], [32], [34], [62].

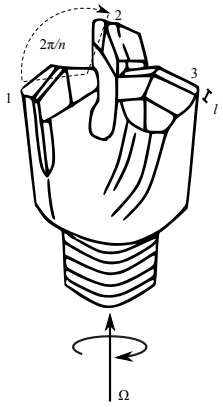

Figure 9: Three blade drag bit.

Consider a drag bit composed by n radial blades regularly spaced by an angle equal to $2\pi/n$. When such a bit is drilling rock, the depth of cut per blade d_n (i.e., the thickness of the rock ridge in front of the blade) is constant along the blade and identical for each blade. Furthermore, d_n is related to the

[3]A drag bit is a specific type of cutting device consisting of n identical blades symmetrically distributed around the axis of revolution.

axial position of the bit U_b according to

$$d_n(t) = U_b(L,t) - U_b(L,t-t_n),$$

where t_n is the time required for the bit to rotate by an angle $2\pi/n$ to its current position at time "t", as schematically illustrated in Figure 9. The delay $t_n(t)$ is a solution of

$$\Phi_b(L,t) - \Phi_b(L,t-t_n) = 2\pi/n. \tag{53}$$

The range of t_n is given by $t_{n_0} = 2\pi/(n\Omega_0)$, with Ω_0 a nominal rotating speed at the top. The combined bit depth of cut is simply $d(t) = nd_n(t)$ or

$$d(t) = n\left[U_b(L,t) - U_b(L,t-t_n)\right]. \tag{54}$$

The torque T and the weight on bit W in the torsional-axial drilling models given in (4), (5) and (6) are functions of the history of Φ_b and of the history of U_b.

An investigation on the drilling response of drag bits was presented in [22]. Detounay and Defourny studied the relations between the weight on bit, the torque, the angular velocity and the rate of penetration. Inspired by the idea that the bit-rock interaction is characterized by the coexistence of rock cutting and frictional contact [30], the torque T and the weight on bit W are decomposed into two components associated with these basic processes. By postulating that the cutting component of T and W is proportional to the depth of cut per revolution, and that a linear constraint exists between the frictional component of T and W, a linear relation is derived between the specific energy and the drilling strength.

Decomposing T and W into a contribution associated to the forces transmitted by the pure cutting process of each cutter (denoted by the subscript c) and another term corresponding to the forces arising from the frictional contact (denoted by the subscript f) we can write:

$$T = T_c + T_f, \qquad W = W_c + W_f.$$

Next, the cutting and friction elements of the above expression are characterized.

FrictionForce/Moment. The frictional elements T_f and W_f are related according to:

$$2T_f(t) = \mu R_b \kappa W_f(t).$$

In [74], these components are modeled as follows:

$$T_f(t) = \frac{R_b^2}{2}\,\kappa\mu\varsigma l\,\mathcal{F}(\|V_b(L,t)\|), \qquad W_f(t) = R_b l\varsigma\,\mathcal{F}(\|V_b(L,t)\|),$$

where R_b is the bit radius, l the length of the wearflat, ς the contact stress, κ is a bit geometry number, greater than 1, that characterizes the orientation and spatial distribution of the frictional contact surfaces associated with the cutters, μ is a coefficient of friction related to the internal friction angle of the rock [3] (ratio between the horizontal and the vertical components of the frictional force), $V_b = (\frac{\partial U_b}{\partial t}, \frac{\partial \Phi_b}{\partial t})$ and $\mathrm{sgn}(V_b)$ designate the orientation of V_b with respect to the horizontal plane, and $\mathcal{F}$ is an dimensionless friction function which can be approximated by the following model, proposed in [74]:

$$\mathcal{F}(x) = \frac{\alpha_0 x}{\sqrt{x^2+\epsilon^2}}, \quad \alpha_0 > 0.$$

In [34] a different approximation for $\mathcal{F}(x)$ is proposed:

$$\mathcal{F}(x) = \frac{1+\mathrm{sgn}(x)}{2}.$$

Alternatively, in [73], the following model is considered:

$$\mathcal{F}(x) = \alpha_0\left(\tanh(x) + \frac{x}{1+\alpha_1 x^2}\right), \quad \alpha_0 > 0, \alpha_1 > 0.$$

Cutting Force/Moment. In [22], the cutting components of the torque T_c and weight W_c are modeled as:

$$T_c(t) = \frac{R_b^2}{2}\,\epsilon d(t), \qquad W_c(t) = R_b \upsilon \epsilon d(t), \tag{55}$$

where υ is a number characterizing the orientation of the cutting force (the ratio of the vertical to the horizontal force for a sharp cutter) and ϵ is the intrinsic

specific energy which is a significant measure of drilling performance, especially of the cutting efficiency of bits and rock hardness. It quantifies a complex process of rock destruction and generally depends on various factors, such as rock type, the rake angle of the cutter, the cutter material, and pressure on the rock surface [69]. The intrinsic specific energy is defined as the energy required to remove a unit volume of rock [71]. In 1982, Rabia concluded that the specific energy is not a fundamental intrinsic property of rocks [59], however, Reddish and Yasar [61], Detournay [23] and Ersoy [28] have found the correlation of the specific energy to the rock properties such as compressive strength and hardness of the rock. In a given drilling environment, a lower ϵ entails a more efficient drilling process.

In [74], T_c is approximated by:

$$T_c(t) = -a_4(\mathcal{F}(\|V_b(L,t)\|)))^2 d(t).$$

where a_4 is a constant related to the Young modulus.

Notice that, according to the considered frictional interface, equations given in (4), (5) and (6) constitute retarded dynamic models characterized by a state-dependent delay t_n.

4. Friction-driven drilling vibrations

It is well known that the proper choice of a friction model guarantees an effective reproduction of the stick-slip and bit-bounce phenomena. In this section, this fact is highlighted through simulations of the drilling system under different rock-bit frictional interface models.

Consider the pair of coupled neutral-type time-delay equations describing the torsional and axial drilling dynamics given in (26)-(28).

The simulations presented below are developed by considering the numerical parameters given in Table 3.

Firstly, let us consider a linear model of the frictional torque $T\Big(\dot{\Phi}_b(t)\Big)$:

$$T\Big(\dot{\Phi}_b(t)\Big) = T_0\dot{\Phi}_b(t). \tag{56}$$

Table 3: Numerical values of the drilling system parameters.

Symbol	**Parameter**	**Numerical value**
L	String length	1172 m
G	Shear modulus	79.3×10^9 N m^{-2}
E	Young modulus	200×10^9 N m^{-2}
Γ	Drillstring's cross-section	35×10^{-4} m^2
J	Second moment of area	1.19×10^{-5} m^4
I	Inertia	0.095 Kg m
I_B	Lumped inertia at the BHA	89 Kg m^2
M_B	Mass at the BHA	40000 Kg
ρ_a	Density	8000 Kg m^{-3}
β	Angular momentum	2000 N m s
α	Viscous friction coefficient	200.025 Kg s^{-1}
c_b	Damping constant	0.03 N m s rad^{-1}
R_b	Bit radius	0.155575 m
W$_{ob}$	Weight on the bit	97347 N
μ_{cb}	Coulomb friction coefficient	0.5
μ_{sb}	Static friction coefficient	0.8
γ_b	Velocity decrease rate	0.9
Ω_0	Angular velocity imposed at the surface	10 rad s^{-1}
ρ_0	Axial velocity imposed at the surface	0.1 m s^{-1}

Figure 10 shows the axial and torsional trajectories of the drill bit when the linear torque on bit friction model (56) is considered. Notice that although torsional vibrations can be observed, the stick-slip phenomenon is not reproduced.

Consider now the velocity weakening law:

$$T(\dot{U}_b, \dot{\Phi}_b) = \zeta \dot{U}_b \mathrm{e}^{-\bar{\alpha}\dot{\Phi}_b}, \tag{57}$$

where ζ is a constant related to the rock hardness.

Using the friction model (57), which considers an exponential decaying term,

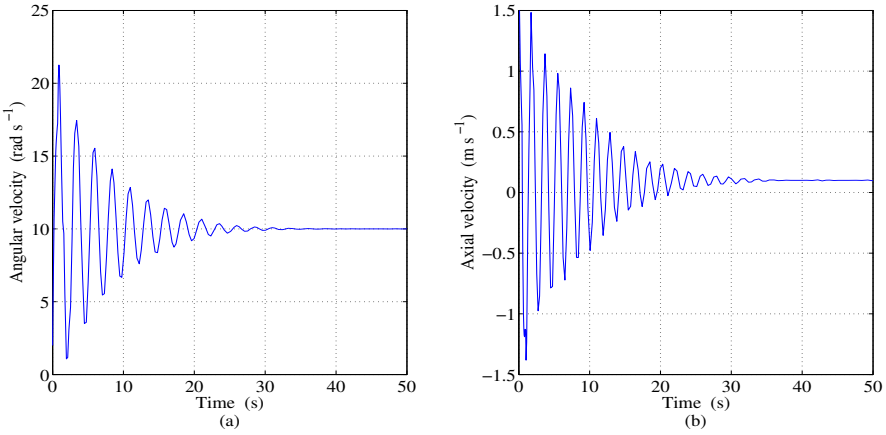

Figure 10: Simulation of model (26)-(28) under the linear model of the frictional torque on bit (56) for $T_0 = 25$ Nms rad^{-1}. (a) Bit angular velocity. (b) Bit axial velocity.

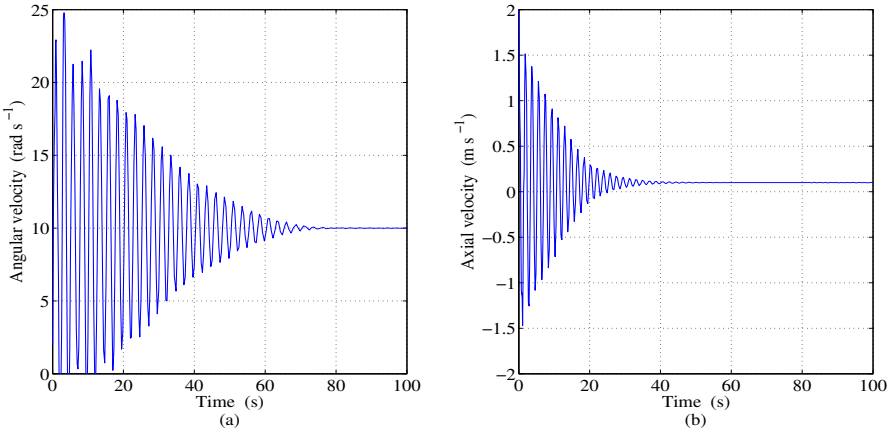

Figure 11: Simulation of model (26)-(28) under the velocity weakening law (57) describing the frictional torque on bit for $\zeta = 650$Ns and $\bar{\alpha} = 0.1$. (a) Bit angular velocity. (b) Bit axial velocity.

the stick-slip behavior can be observed within the first few seconds of the simulation, see Figure 11.

A more sophisticated model to describe the rock-bit interaction is given by

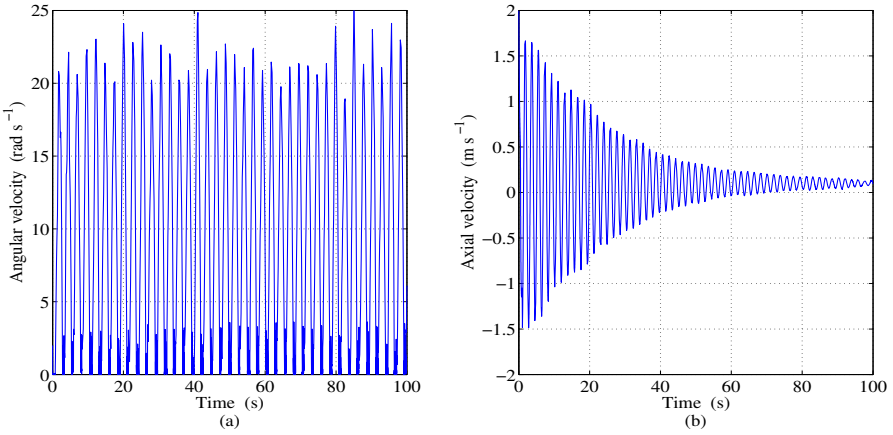

Figure 12: Simulation of model (26)-(28) subject to the Karnopp-type friction function with a decaying term (58)-(50). (a) Bit angular velocity. (b) Bit axial velocity.

the following nonlinear function, derived from the Karnopp's models given in Sections 3.4 and 3.5:

$$T\left(\dot{\Phi}_b(t)\right) = c_b\dot{\Phi}_b(t) + W_{ob}R_b\mu_b\left(\dot{\Phi}_b(t)\right)\operatorname{sgn}\left(\dot{\Phi}_b(t)\right). \tag{58}$$

The term $c_b\dot{\Phi}_b(t)$ represents the viscous damping torque at the bottom end and the expression $W_{ob}R_b\mu_b\left(\dot{\Phi}_b(t)\right)\operatorname{sgn}\left(\dot{\Phi}_b(t)\right)$ approximates the dry friction torque. The notations R_b and W_{ob} stand for the bit radius and the weight on bit, respectively. The friction coefficient $\mu_b(\dot{\Phi}_b(t))$ can be approximated by the decaying term (50) or the exponential decaying expression given in (51).

Simulations of the drilling system model (26)-(28) subject to the friction torque model (58) for μ_b given in (50) and in (51) are shown in Figures 12 and 13, respectively. Observe that the responses are quite similar due to the affinity of the friction torque models. The angular velocity varies between zero and twice the reference velocity $\Omega_0 = 10\text{rad s}^{-1}$, which clearly characterizes the stick-slip phenomenon.

As reviewed before, the frictional torque on bit can be approximated by the function (52); a simulation of the drilling system allows assessing the accuracy

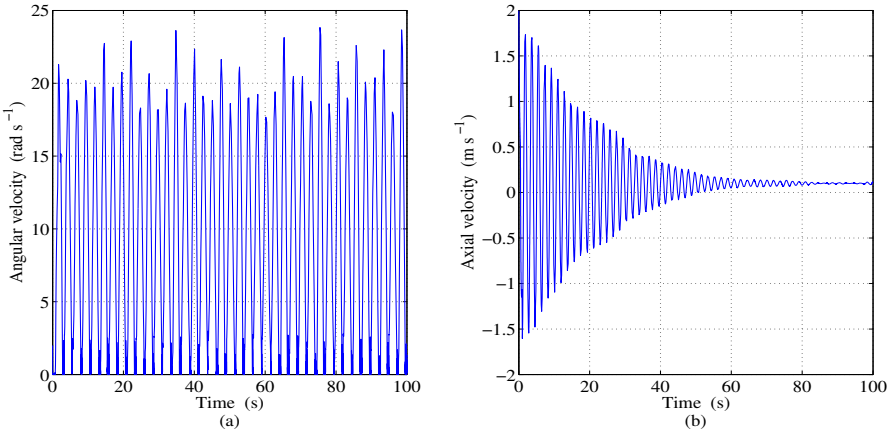

Figure 13: Simulation of model (26)-(28) subject to the Karnopp-type friction function with an exponential decaying term (58)-(51). (a) Bit angular velocity. (b) Bit axial velocity.

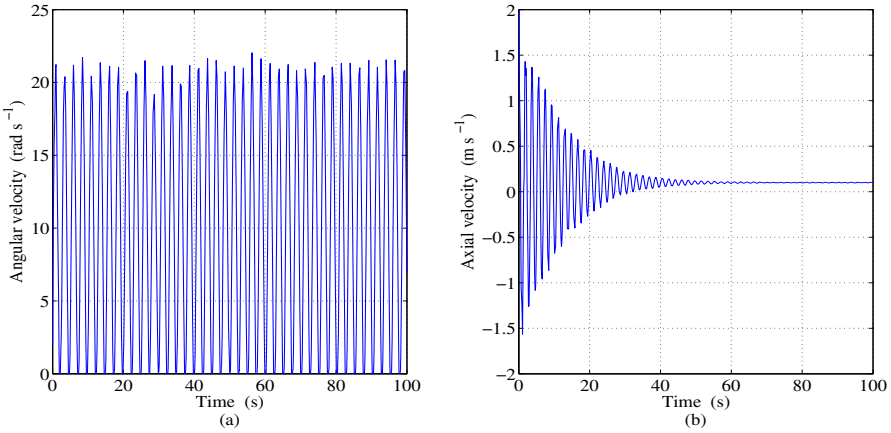

Figure 14: Simulation of model (26)-(28) under the simplified frictional torque on bit model (59) for $p = 1000$. (a) Bit angular velocity. (b) Bit axial velocity.

of this simplified model. Figure 14 shows the angular and axial bit trajectories for a frictional model of the form:

$$T(\dot{\Phi}_b(t)) = \frac{2p\bar{k}\dot{\Phi}_b(t)}{\dot{\Phi}_b^2(t) + \bar{k}^2}, \quad p > 0,\ \bar{k} > 0. \tag{59}$$

In this context, it is important to point out that the similarity between the bit trajectories depicted in Figures 12, 13 and 14 is remarkable.

5. Concluding remarks

The presence of self-excited vibrations provokes the premature failure of the drilling system components and delays the overall process leading to a significant increase of costs. The prediction of erratic behaviors and the design of controllers for the suppression of drilling vibration requires a suitable model of the system dynamics.

Over the last half century, drillstring vibration models have been improved to accurately predict an erratic behavior and determine the effect of manipulable parameters such as the rotary speed, the torque, and the weight on bit on the drillstring vibrations. The extreme complexity of the physical phenomena occurring during the perforation process in oilwells makes the modeling of drilling vibrations a very difficult task. Models are limited by determined assumptions and simplifications; multiple system elements are considered unknown or uncertain. Accuracy of the models depends on the proximity to the reality of the considered assumptions regarding the geometric aspects of the drillstring configuration, excitation sources, damping effects, rock-bit interface, among others. Despite the challenges posed by its construction, mathematical modeling are a powerful and emerging method to investigate the propagation of vibrations along the drillstring. The development of upgraded models is necessary for an effective prediction of downhole vibrations, their economical interest has been renewed by recent oilfields discoveries and the development of new drilling techniques leading to a growing literature.

In this paper, some time-domain modeling techniques that allow the oscillatory behavior analysis of the physical system have been reviewed. Formulations of distributed parameter models, lumped parameter models, neutral-type time-domain models and coupled PDE-ODE models encountered in the literature have been presented, their benefits and limitations have been outlined. A liter-

ature review on the research objectives pursued with each modeling approach were presented.

Bibliography

[1] Aarrestad, T.V., Tonnesen, H.A., Kyllingstad, A. (1986). Drillstring vibrations: comparison between theory and experiments on a full-scale research drilling rig. SPE/IADC SPE-14760-MS, Society of Petroleum Engineers.

[2] Aarsnes, U.J.F., Aamo, O.M. (2016). Linear stability analysis of self-excited vibrations in drilling using an infinite dimensional model. *Journal of Sound and Vibration* 360(6), 239–259.

[3] Adachi, J.I., Detournay, E., Drescher, A. (1996). Determination of rock strength parameters from cutting tests. *Proceedings 2nd North American Rock Mechanics Symposium*, Balkema, Rotterdam, 1517–1523.

[4] Bailey, J.J., Finnie, I. (1960). An analytical study of drillstring vibration. *Journal of Engineering for Industry, Transactions of the ASME*, 82(2), 122–128.

[5] Balanov, A.G., Janson, N.B., McClintock, P.V.E., Wang, C.H.T. (2002). Bifurcation analysis of a neutral delay differential equation modelling the torsional motion of a driven drill-string. *Chaos, Solitons and Fractals*, 15(2), 381–394.

[6] Besselink, B., van de Wouw, N., Nijmeijer, H. (2011). A semi-analytical of stick-slip oscillations in drilling systems, *ASME Journal of Computational and Nonlinear Dynamics*, 6(2), 021006-1–021006-9.

[7] Borg, S.F. (1962). Fundamentals of engineering elasticity. Van Nostrand.

[8] Boussaada, I., Mounier, H., Niculescu, S.I., Cela, A. (2012). Analysis of drilling vibrations: a time delay system approach. *20th Mediterranean Conference on Control and Automation MED*, Barcelona, Spain.

[9] Boussaada, I., Cela, A., Mounier, H., Niculescu, S.I. (2013). Control of drilling vibrations: a time-delay system-based approach *11th Workshop on Time-Delay Systems Part of 2013 IFAC Joint Conference SSSC*, Grenoble, France.

[10] Boussaada, I., Saldivar, B., Mounier, H., Niculescu, S.I. (2016). Delay system modeling of rotary drilling vibrations. Springer - Recent results on time-delay systems: analysis and control. Advances in Delays and Dynamics, 5, 23–44.

[11] Bresch-Pietri, D., Krstic, M. (2014). Output-feedback adaptive control of a wave PDE with boundary anti-damping. *Automatica*, 50, 1407–1415.

[12] Bresch-Pietri, D., Krstic, M. (2014). Adaptive output feedback for oil drilling stick-slip instability modeled by wave PDE with anti-damped dynamic boundary. *Proceedings of the American Control Conference 2014* (Invited Session), Portland, OR, USA.

[13] Bresch-Pietri, D., Krstic, M. (2014). Adaptive output-feedback for wave PDE with anti-damping – application to surface-based control of oil drilling stick slip instability. *Proceedings of the 2014 Conference on Decision and Control*, Los Angeles, CA, USA.

[14] Brett, J.F. (1992). The genesis of torsional drillstring vibrations. SPE Drilling Engineering, 7(3), 168–174.

[15] Canudas-de-Wit, C., Rubio, F.R., Corchero, M.A. (2008). D-OSKIL: a new mechanism for controlling stick-slip oscillations in oil well drillstrings. *IEEE Transactions on Control Systems Technology*, 16(6), 1177–1191.

[16] Challamel, N. (2000). Rock destruction effect on the stability of a drilling structure. *Journal of Sound and Vibration,* 233(2), 235–254.

[17] Clayer, F., Vandiver, J.K., Lee, H.Y. (1990). The effect of surface and downhole boundary conditions on the vibration of drillstrings. *65th An-*

nual Technical Conference and Exhibition of the Society of Petroleum Engineers, 431–442.

[18] Christoforou, A.P., Yigit, A.S. (2003). Fully coupled vibrations of actively controlled drillstrings. *Journal of Sound and Vibration,* 267(5), 1029–1045.

[19] Cull, S.J., Tucker, R.W. (1999). On the modelling of Coulomb friction. *Journal of Physics A: Mathematical and General*, 32(11), 2103–2113.

[20] Depouhon, A., Detournay, E. (2014). Instability regimes and self-excited vibrations in deep drilling systems. *Journal of Sound and Vibration*, 333(7), 2019–2039.

[21] Detournay, E., Atkinson, C. (2000). Influence of pore pressure on the drilling response in low-permeability shear-dilatant rocks. *International Journal of Rock Mechanics and Mining Sciences*, 37(7), 1091-1101.

[22] Detournay, E., Defourny, P. (1992). A phenomenological model for the drilling action of drag bits. *International Journal of Rock Mechanics, Mining Science and Geomechanical Abstracts* 29, 13–23.

[23] Detournay, E. Tan, C.P. (2002). Dependence of drilling specific energy on bottom-hole pressure in shales. SPE/ISRM 78221, Rock Mechanics Conference, Irving, Texas.

[24] Di Meglio, F., Aarsnes, U.J.F. (2015). A distributed parameter systems view of control problems in drilling. *2nd IFAC Workshop on Automatic Control in Offshore Oil and Gas Production*, Florianpolis, Brazil.

[25] Doebelin, E. O. (1998).System dynamics: modeling, analysis, simulation, design. Marcel Dekker, Inc.

[26] Dunayevsky, V., Abbassian, F., Judzis, A. (1993). Dynamic stability of drillstrings under fluctuating weight on bit. *SPE Drilling and Completion*, 8(2), 84–92.

[27] Egeland, O., Gravdahl, J. (2002). Modeling and Simulation for Automatic Control. Marine Cybernetics, Trondheim, Norway.

[28] Ersoy, A. (2003). Automatic drilling control based on minimum drilling specific energy using PDC and WC bits. *Transactions of the Institution of Mining and Metallurgy*, Section A: Mining Technology, 112, 86–96.

[29] Ertas, D., Bailey, J.R., Wang, L., Pastusek, P.E. (2013). Drillstring mechanics model for surveillance, root cause analysis, and mitigation of torsional and axial vibrations. *Proceedings of the SPE/IADC Drilling Conference and Exhibition*, 203–216, Amsterdam, The Netherlands.

[30] Fairhurst C., Lacabanne W. D. (1957). Mine and Quarry Engineering, 157–161, 194–197.

[31] Finnie, I., Bailey, J.J. (1960). An experimental study of drill-string vibration. *Journal of Engineering for Industry, Transactions of the ASME*, 82(2), 129–135.

[32] Germay, C. (2009). Modeling and analysis of self-excited drill bit vibrations. PhD dissertation, University of Liège.

[33] Germay, C., Denoël, V., Detournay, E. (2009). Multiple mode analysis of the self-excited vibrations of rotary drilling systems. *Journal of Sound and Vibration*, 325(1-2), 362–381.

[34] Germay, C., Van De Wouw, N., Nijmeijer, H., Sepulchre, R. (2005). Nonlinear drilling dynamics analysis. *SIAM Journal on Applied Dynamical Systems*, 8(2), 527–553.

[35] Germay, C., Van De Wouw, N., Sepulchre, R., Nijmeijer, H. (2005). Axial stick-slip limit cycling in a drill-string model with delay. *Proceedings of the 5th Euromech nonlinear dynamics conference*, Eindhoven, 2005.

[36] Ghasemloonia, A., Rideout, D.G., Butt, S.D. (2015). A review of drillstring vibration modeling and suppression methods. *Journal of Petroleum Science and Engineering*, 131, 150–164.

[37] Graff, K.F. (1975). Wave motion in elastic solids. Dover publications Inc. New York.

[38] , Hakimi, H., Moradi, S., (2009). Drillstring vibration analysis using differential quadrature method. *Journal of Petroleum Science and Engineering*, 70, 235–242.

[39] Halsey, G.W., Kyllingstad, A., Kylling, A. (1988). Torque feedback used to cure slip-stick motion. *Proceedings of the 63rd Society of Petroleum Engineers Drilling Engineering*, Annual Technical Conference and Exhibition, Houston, TX, 277–282.

[40] Henneuse, H. (1992). Surface detection of vibrations and drilling optimization: field experience. *Proceedings of IADC/SPE Drilling Conference*, New Orleans, Lousiana, 409–423.

[41] Insperger, T., Stépán, Turi, J. (2006). State-dependent delay in regenerative turning processes. *Nonlinear Dynamics*, 47(1-3), 275–283.

[42] Jansen, J.D., van den Steen L. (1995). Active damping of self-excited torsional vibrations in oil well drillstrings. *Journal of Sound and Vibration,* 179(4), 647–668.

[43] Kamel, J.M., Yigit, A.S. (2014). Modeling and analysis of stick-slip and bit bounce in oil well drillstrings equipped with drag bits. *Journal of Sound and Vibration,* 333, 6885–6899.

[44] Karnopp, D. (1985). Computer simulation of stick-slip friction in mechanical dynamic systems. *Transactions of the ASME Journal of Dynamic Systems, Measurement and Control*, 107 (1), 100–103.

[45] Khalil, H.K. (2002). Nonlinear systems, 3rd Edition, Prentice hall Upper Saddle River.

[46] Khulief, Y.A., Al-Sulaiman, F.A., Bashmal, S. (2007). Vibration analysis of drillstrings with self-excited stick-slip oscillations. *Journal of Sound and Vibration*, 299, 540–558.

[47] Knüppel, T., Woittennek, F., Boussaada, I., Mounier, H., Niculescu, S.I. (2013). Flatness-based control for a non-linear spatially distributed model of a drilling system. *Low Complexity Controllers for Time Delay Systems*, Springer ser. Adv. in Delays and Dynamics, 2013.

[48] Leine, R.I. (1997). Literature survey on torsional drillstring vibrations. Report number: WFW 97.069, Division of Computational and Experimental Mechanics, Department of Mechanical Engineering Eindhoven University of Technology, The Netherlands.

[49] Liao, C., Balachandran, B., Karkoub, M., Abdel-Magid, Y.L. (2011). Drill-string dynamics: reduced-order models and experimental studies. *Journal of Vibration and Acoustics*, 133(4), ID 041008.

[50] Lin, Y., Wang, Y. (1991). Stick-slip vibration of drill strings. *Transactions of ASME*, 113, 38–43.

[51] Liu, X., Vlajic, N., Long, X., Meng, G., Balachandran, B. (2013). Nonlinear motions of a flexible rotor with a drill bit: stick-slip and delay effects. *Nonlinear Dynamics*, 72(1–2), 61–77.

[52] Macpherson, J.D., Mason, J.S., Kingman, J.E.E. (1993). Surface measurement and analysis of drillstring vibrations while drilling. SPE/IADC 25777, Society of Petroleum Engineers.

[53] Mason, J.S., Sprawls, B.M. (1998). Addressing BHA whirl: the culprit in mobile bay. SPE Drilling and Completion, 13(4), 231–236.

[54] Mitchell, R.F., Allen, M.B. (1987). Case studies of BHA vibration failure. SPE 16675, Society of Petroleum Engineers.

[55] Nandakumar, K., Wiercigroch, M. (2013). Stability analysis of a state dependent delayed, coupled two DOF model of drill-string vibration. *Journal of Sound and Vibration*, 332, 2575–2592.

[56] Navarro-López, E., Cortés, D. (2007). Sliding-mode of a multi-DOF oilwell drillstring with stick-slip oscillations. *Proceedings of the 2007 American Control Conference*. New York City, USA, 3837–3842.

[57] Navarro-López, E., Suárez, R. (2004). Practical approach to modelling and controlling stick-slip oscillations in oilwell drillstrings. *Proceedings of the 2004 IEEE International Conference on Control Applications*, 1454–1460.

[58] Patil P.A., Teodoriu, C. (2013). A comparative review of modelling and controlling torsional vibrations and experimentation using laboratory setups. *Journal of Petroleum Science and Engineering*, 112, 227–238.

[59] Rabia H. (1982). Specific energy as a criterion for drilling performance prediction. *International Journal of Rock Mechanics and Mining Sciences*, 19, 39–42.

[60] Rasvan, V. (1975). A method for distributed parameter control systems and electrical networks analysis. *Rev. Roumaine Sci. Techn. Serie Electrotechn. Energ.* 20, 561–566.

[61] Reddish, D.J., Yasar, E. (1996). A new portable rock strength index test based on specific energy of drilling. *International Journal of Rock Mechanics Mining Sciences & Geomechanics*. 33(5), 543–548.

[62] Richard, T., Germay, C., Detournay E. (2007). A simplified model to explore the root cause of stickslip vibrations in drilling systems with drag bits. *Journal of Sound and Vibration*, 305, 432–456.

[63] Sagert, C., Di Meglio, F., Krstic, M., Rouchon, P. (2013). Backstepping and flatness approaches for stabilization of the stick-slip phenomenon for drilling. *IFAC Symposium on System Structure and Control*, Grenoble, France.

[64] Saldivar, M.B., Mondié, S., Loiseau, J.J. (2009). Reducing stick-slip oscillations in oilwell drillstrings. *6th International Conference on Electrical*

Engineering, Computing Science and Automatic Control (CCE), Toluca, México, 1–6.

[65] Saldivar, B., Mondié, S. Loiseau, J.J., Rasvan, V. (2013). Suppressing axial torsional coupled vibrations in oilwell drillstrings. *Journal of Control Engineering and Applied Informatics*, 15(1), 3–10.

[66] Saldivar, M.B., Mondié S. (2013). Drilling vibration reduction via attractive ellipsoid method. *Journal of the Franklin Institute - Elsevier*, 350(3), 485–502.

[67] Saldivar, B., Boussaada, I., Mounier, H., Mondié, S., Niculescu, S.I. (2014). An overview on the modeling of oilwell drilling vibrations. *19th World Congress of the International Federation of Automatic Control*, Cape Town, South Africa.

[68] Sarker, M., Rideout, D.G., Butt, S.D. (2012). Dynamic model of an oilwell drillstring with stick-slip and bit-bounce interaction. *International Conference on Bond Graph Modeling ICBGMS'12*, Genoa, Italy.

[69] Shewalla, M. (2007). Evaluation of shear strength parameters of shale and siltstone using single point cutter tests. M. Sc. Thesis. Graduate Faculty of the Louisiana State University and Agricultural and Mechanical College.

[70] Serrarens, A.F.A., van de Molengraft, M.J.G., Kok, J.J., van den Steeen, L. (1998). $\mathcal{H}_\infty$ control for suppressing stick-slip in oil well drillstrings. *IEEE Control Systems*, 18(2), 19–30.

[71] Teale, R. (1965). The concept of specific energy in rock drilling. *International Journal of Rock Mechanics & Mining Sciences*. 2, 57–73.

[72] Tucker, R.W., Wang, C. (1999). On the effective control of torsional vibrations in drilling systems. *Journal of Sound and Vibration*, 224(1), 101–122.

[73] Tucker R.W., Wang, C. (2000). The excitation and control of torsional slip-stick in the presence of axial vibrations. Citeseer Computer and Information Science Publications collection. Id. 41923656.

[74] Tucker, R.W., Wang, C. (2003). Torsional vibration control and Cosserat dynamics of a drill-rig assembly. *Mecanica*, 38(1), 145–161.

[75] Vandiver, J.K., Nicholson, J.W., Shyu, R.J. (1990) Case studies of the bending vibration and whirling motion of drill collars. SPEDE, SPE 18652, 282–290.

[76] Villafuerte, R., Saldivar, B., Mondié, S. (2013). Practical stability and stabilization of a class of nonlinear neutral type time delay systems with multiple delays: BMI's approaches. *International Journal of Control, Automation and Systems*, 11(5), 859–867.

[77] Vromen, T.G.M. (2015). Control of stick-slip vibrations in drilling systems. PhD thesis, Eindhoven University of Technology, Eindhoven, the Netherlands.

[78] Yigit, A.S., Christoforou, A.P. (2006). Stick-slip and bit-bounce interaction in oil-well drillstrings. *Journal of Energy Resources Technology*, 128(4), 268–274.